A Comparison of Techniques for State-Space Transient Analysis of Transmission Lines

Jose A. Rosendo Macías, *Member, IEEE*, Antonio Gómez Expósito, *Fellow, IEEE*, and Alfonso Bachiller Soler, *Member, IEEE*

***Abstract*—This paper reviews and compares several methods to analytically obtain the transient response of transmission lines in the time domain, in those cases where frequency independent parameters can be assumed. The distributed-parameter line is modeled by the cascaded connection of a number of lumped-parameter π circuits, each one representing a fraction of the line length, leading to a linear time-invariant (LTI) circuit.**

The associated state-space equations are formulated, allowing explicit expressions for the state variables to be written in the time domain. The solution is then obtained by means of three different approaches, all of them requiring that the natural frequencies be previously computed, namely: eigenvector-based procedure, Vandermonde matrix method, and Lagrange interpolation formula. Numerical integration by the trapezoidal rule is also considered for comparison.

Two kinds of test results are presented. First, accuracy of the results provided by the LTI lumped-parameter model are compared with those obtained using the Electromagnetic Transients Program. Second, a comparison is performed in terms of the computational cost involved in each method. Two cases of practical interest are assessed, namely solving from scratch the state equations and updating the solution for a new set of initial conditions.

***Index Terms*—Natural response, state variables, transient analysis, transmission lines.**

I. Introduction

ACCURATE determination of transmission line transients, as a result of faults and switching operations, is necessary for the design of protective devices and selection of adequate insulation levels.

The distributed nature of transmission line parameters and their frequency dependence makes it very difficult to obtain the solution in the time domain.

Depending on the application and underlying assumptions, a number of methods are available to obtain electromagnetic line transients. Among these, the following techniques can be cited: traveling wave methods (lattice diagram and Bergeron) [1], Electromagnetic Transients Program (EMTP) [2], and Laplace or Fourier transforms [3], [4]. In those cases where frequency dependence of line parameters can be ignored, numerical integration of the state-space equations provided by a simplified lumped-parameter model has been also proposed [5].

Manuscript received March 15, 2004; revised June 7, 2004. Paper no. TPWRD-00136-2004.

The authors are with the Department of Electrical Engineering, University of Sevilla, 41092 Sevilla, Spain (e-mail: rosendo@esi.us.es).

Digital Object Identifier 10.1109/TPWRD.2005.844271

In this paper, the state-space approach, by which the line is modeled with a number of cascaded π networks, is also adopted. In addition to the trapezoidal integration rule considered in [5], this paper explores several techniques for the explicit solution of the associated state-space equations. Results provided by the cascaded connection of lumped-parameter circuits are compared in terms of accuracy with those provided by the EMTP, the standard tool for the analysis of fast transients in power systems. Furthermore, a detailed analysis of the computational cost involved in each method is performed.

Clearly, the state-space formulation adopted for transient analysis is of application to generic linear circuits, provided all distributed-parameter elements are replaced by a sufficiently large number of lumped-parameter sections. However, the analysis is intentionally restricted in this paper to the single line case, the cascaded connection of lines and/or cables being a trivial extension. On the one hand, these simple cases lead to equation systems with tridiagonal structure, allowing explicit expressions for the computational cost to be obtained. On the other hand, a few classical and more recent applications can be cited where the analysis of cascaded devices (circuit breakers, shunt capacitor banks, transformers, lines, and cables) can be of practical interest, namely:

- Insulation coordination of very high voltage systems, in which switching transients play an important role [6]–[8]. This includes assessment of new arrangements and equipment associated with switching devices, like single-pole switching for capacitor banks, resistor insertion in multistage circuit breakers, etc. In this context, it has been stated that a reduction of 0.2 pu in switching overvoltages may lead to economic benefits when selecting insulation equipment [3].
- Lightning surge propagation and attenuation [9].
- Test and assessment of more sophisticated digital protective relaying algorithms [10]–[12].

The paper is organized as follows: the EMTP line model is introduced in Section II and the application of the cascaded nominal π circuit for transient analysis is discussed in Section III. The state-space model of transmission lines is then presented in Section IV and the solution methods considered in this paper are introduced in Section V. An example is studied in Section VI and the computational cost is compared in Section VII. Section VIII is devoted to the common case in which the analysis is repeated for different initial conditions. Finally, conclusions are drawn in Section IX.

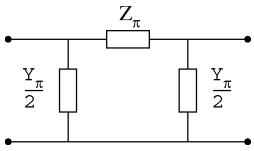

Fig. 1. Equivalent π circuit for steady-state analysis.

II. EMTP Line Models

A. Steady-State Model

For frequency-domain steady-state analysis, both at the fundamental and harmonic frequencies, the transmission line can be accurately modeled by the π circuit shown in Fig. 1.

The equivalent lumped parameters of Fig. 1 are given by:

$$Z_\pi = (Z\ell)\frac{\sinh(\gamma\ell)}{\gamma\ell}$$
$$Y_\pi = (Y\ell)\frac{\tanh\left(\frac{\gamma\ell}{2}\right)}{\frac{\gamma\ell}{2}}$$
$$\gamma = \sqrt{ZY} \tag{1}$$

where Z and Y represent the series impedance and shunt admittance per unit length, respectively,

$$Z = R + j\omega L$$
$$Y = G + j\omega C \tag{2}$$

and ℓ is the line length.

For medium length lines the equivalent π circuit shown in Fig. 1 tends to the so-called "nominal π circuit," with

$$Z_\pi \approx Z\ell \quad Y_\pi \approx Y\ell. \tag{3}$$

B. Transient Model

In addition to the explicit frequency dependence of the above expressions, the line parameters are also functions of frequency. Owing to this two-fold frequency dependence, the equivalent π circuit has no counterpart in the time domain. For time-domain simulations, several alternative models exist [13], all of them based on the decoupling introduced between the sending and receiving ends by the wave traveling time.

The EMTP lossless line model is based on the Bergeron's traveling wave method [2]. In this ideal model, the single-phase distributed LC line is characterized by two values, namely the surge impedance, $Z_c = \sqrt{L/C}$, and the speed of propagation, $v = 1/\sqrt{LC}$.

In a real line, the series losses are taken into account by lumping a resistance of $R\ell/4$ at both ends of the line and a resistance of $R\ell/2$ in the middle. Experience with this model [13] indicates that the error incurred by lumping the series resistance is acceptable as long as $R\ell \ll Z_c$.

A two-port model of the line can be obtained as shown in Fig. 2, where [14]

$$I_s(t) = \left(\frac{1+h}{2}\right)\left[\frac{1}{Z}v_r(t-\tau) + hi_r(t-\tau)\right] + \left(\frac{1-h}{2}\right)\left[\frac{1}{Z}v_s(t-\tau) + hi_s(t-\tau)\right] \tag{4}$$

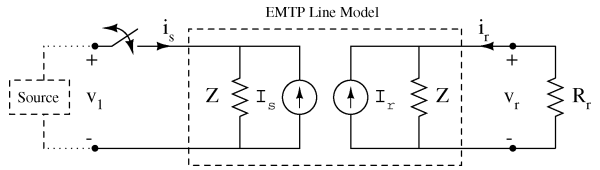

Fig. 2. EMTP transmission line model for time-domain analysis.

$$I_r(t) = \left(\frac{1+h}{2}\right)\left[\frac{1}{Z}v_s(t-\tau) + hi_s(t-\tau)\right] + \left(\frac{1-h}{2}\right)\left[\frac{1}{Z}v_r(t-\tau) + hi_r(t-\tau)\right] \tag{5}$$

$$Z = Z_c + \frac{R\ell}{4}\ ;\ h = \frac{Z_c - \frac{R\ell}{4}}{Z_c + \frac{R\ell}{4}}\ ;\ \tau = \ell\sqrt{LC}. \tag{6}$$

Each integration step involves computing the current sources (4) and (5), building and solving the nodal equations and then updating $i_s(t)$ and $i_r(t)$.

III. Cascaded Nominal π Circuits

When the frequency spectrum of the signals involved in the simulation is not too wide, assuming frequency-independent line parameters constitutes a reasonable simplification. In such cases, cascading nominal π circuits is a simple alternative to approximating the effect of the hyperbolic correction factors for time-domain transient simulations [13].

Fig. 3 shows a given length of line represented by connecting N short nominal π sections in cascade. The parameters of each nominal π network are determined by dividing the total resistance, inductance, conductance and capacitance for the length considered by the number of cascaded networks.

The number of sections to be used depends on the frequency range of concern. A good approximation of the highest frequency range represented by the cascaded nominal π circuits is given by the following equation [15]

$$f_{\max} = \frac{Nv}{\pi\ell}. \tag{7}$$

Fig. 4 compares, for the 220-kV, 100-km line tested in Section VI, the frequency response of the driving-point impedance (receiving end open-circuited) corresponding to the exact π model of Fig. 1 with that of the cascaded connection of 12 lumped π circuits. This diagram indicates that the approximation is acceptable up to the 4–5 kHz range.

Note however that, as explained in [13], [16], when the time step of the simulation is larger than the line traveling time, τ, the use of the nominal π circuit is the only viable alternative.

IV. State Space Model of Transmission Lines

Unlike the distributed parameter line model, the cascaded connection of nominal π circuits leads to a linear state space model with a finite number of states. Each nominal π network contains a series resistance and inductance, and a shunt conductance and capacitance as seen in Fig. 5.

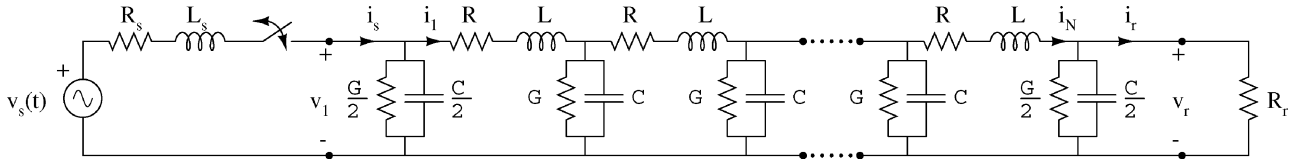

Fig. 3. Transmission line model based on N lumped-parameter π networks.

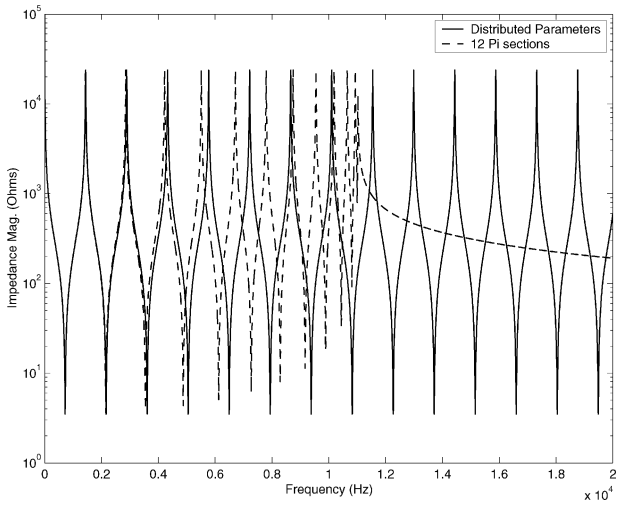

Fig. 4. Driving-point impedance frequency response.

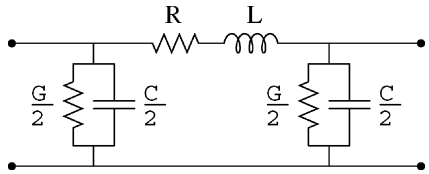

Fig. 5. π network section.

In this model, inductor currents and capacitor voltages constitute state variables. In addition, for a typical configuration like the one shown in Fig. 3, the source inductance current should be added to the state vector (in the same way, an inductance could be added to the load, which is omitted for simplicity). The resulting state equations for the cascaded nominal π circuits shown in Fig. 3 can be written as [5]

$$\dot{\mathbf{x}} = \mathbf{A}_l \mathbf{x} + \mathbf{B}_l v_s \tag{8}$$

where

$$\mathbf{x}^T = [\, i_s \quad v_1 \quad i_1 \quad v_2 \quad i_2 \quad v_3 \quad \ldots \quad i_N \quad v_r \,]$$

and (see (9)–(10) at the bottom of the page).

Note that $\mathbf{A}_l$ is a tridiagonal matrix, whose eigenvalues can be obtained in a straightforward manner.

V. Solution of the State Equations

Consider the linear time-invariant system

$$\dot{\mathbf{x}} = \mathbf{A}\mathbf{x} + \mathbf{B}\mathbf{u} \quad ; \quad \mathbf{x}(0) = \mathbf{x}_0 \tag{11}$$

where $\mathbf{x} \in \mathbb{R}^n$ is the state vector, $\mathbf{u} \in \mathbb{R}^m$ is the excitation vector, and $\mathbf{A} \in \mathbb{R}^{nxn}$, $\mathbf{B} \in \mathbb{R}^{nxm}$ are known coefficient matrices.

Among the long list of methods developed by mathematicians to solve the above set of linear ordinary differential equations [17], the following four, suitable for realistic systems, are selected for comparison in this paper.

$$\mathbf{B}_l^T = [\, \tfrac{1}{L_s} \quad 0 \quad \ldots \quad 0 \,] \tag{9}$$

$$\mathbf{A}_l = \begin{bmatrix}
\frac{-R_s}{L_s} & \frac{-1}{L_s} & & & & & & & \\
\frac{2}{C} & \frac{-G}{C} & \frac{-2}{C} & & & & & & \\
 & \frac{1}{L} & \frac{-R}{L} & \frac{-1}{L} & & & & & \\
 & & \frac{1}{C} & \frac{-G}{C} & \frac{-1}{C} & & & & \\
 & & & \frac{1}{L} & \frac{-R}{L} & \frac{-1}{L} & & & \\
 & & & & \frac{1}{C} & \frac{-G}{C} & \frac{-1}{C} & & \\
 & & & & & \ddots & \ddots & \ddots & \\
 & & & & & & \frac{1}{L} & \frac{-R}{L} & \frac{-1}{L} \\
 & & & & & & & \frac{2}{C} & \frac{-2}{CR_r} - \frac{G}{C}
\end{bmatrix} \tag{10}$$

A. Trapezoidal Rule

By means of the trapezoidal integration rule, a differential equation like (11) is easily converted into a set of discrete-time equations, as follows:

$$\mathbf{x}_{k+1} = \mathbf{x}_k + \frac{\Delta t}{2}[\mathbf{A}(\mathbf{x}_{k+1} + \mathbf{x}_k) + \mathbf{B}(\mathbf{u}_{k+1} + \mathbf{u}_k)] \quad (12)$$

where Δt is the time step and $\mathbf{x}_k$, $\mathbf{u}_k$ refer to the respective magnitudes evaluated at $t = k\Delta t$. Rearranging (12) yields

$$\left(\mathbf{I} - \frac{\Delta t}{2}\mathbf{A}\right)\mathbf{x}_{k+1} = \left(\mathbf{I} + \frac{\Delta t}{2}\mathbf{A}\right)\mathbf{x}_k + \frac{\Delta t}{2}\mathbf{B}(\mathbf{u}_k + \mathbf{u}_{k+1}). \quad (13)$$

Each integration step requires that a tridiagonal linear system be solved, in which the coefficient matrix remains constant so long as the time step is also constant. Note that, at intermediate steps, all components of $\mathbf{x}$ must be computed so that the right-hand side in (13) is fully defined for the next solution. In those cases where only a single state variable is of interest (typically the receiving bus voltage), the back substitution process during the last step is not needed, but this saving is negligible.

B. Eigensystem-Based Solution

This and the remaining procedures require that the eigenvalues of $\mathbf{A}$ be previously computed. For simplicity, it will be assumed that $\mathbf{A}$ has distinct eigenvalues, but the methods described below can be extended to the unlikely case of multiple eigenvalues.

The solution of (11) can be expressed as [18], [19]

$$\mathbf{x} = \mathbf{x}_f + \mathbf{x}_h \quad (14)$$

where $\mathbf{x}_f$ is the forced or steady-state solution of (11), and $\mathbf{x}_h$ is the natural response satisfying the homogeneous system

$$\dot{\mathbf{x}}_h = \mathbf{A}\mathbf{x}_h \quad (15)$$

subject to the initial value

$$\mathbf{x}_h(0) = \mathbf{x}_0 - \mathbf{x}_f(0).$$

The natural response has the generic form [20]

$$\mathbf{x}_h(t) = \sum_{j=1}^{n} \alpha_j e^{\lambda_j t}\mathbf{T}_j \quad (16)$$

where λ_j are the eigenvalues of $\mathbf{A}$ (natural complex frequencies), $\mathbf{T}_j$ are arbitrarily scaled eigenvectors and α_j are scalars selected in such a way that the initial conditions are satisfied, that is

$$\mathbf{x}_h(0) = \sum_{j=1}^{n} \alpha_j \mathbf{T}_j. \quad (17)$$

If $\mathbf{T} = [\mathbf{T}_1, \mathbf{T}_2, \ldots, \mathbf{T}_n]$ denotes the similarity transformation matrix comprising the whole set of eigenvectors, the above system can be written in matrix form as follows:

$$\mathbf{T}\boldsymbol{\alpha} = \mathbf{x}_h(0) \quad (18)$$

where $\boldsymbol{\alpha} = [\alpha_1, \alpha_2, \ldots, \alpha_n]^T$. Note that, unlike in (13), the coefficient matrix $\mathbf{T}$ is dense, i.e., all its elements are nonnull. Each column $\mathbf{T}_j$ is previously obtained in a decoupled manner by solving the homogeneous system

$$(\mathbf{A} - \lambda_j\mathbf{I})\mathbf{T}_j = 0\ ,\ j = 1, 2, \ldots, n. \quad (19)$$

Some computational saving is possible if a single state variable x_i is of interest, as each α_j coefficient needs to be multiplied only by T_{ij}, rather than by the entire column vector $\mathbf{T}_j$.

C. Vandermonde Matrix

Instead of separately obtaining α_j and $\mathbf{T}_j$, the following scaled eigenvector:

$$\mathbf{C}_j = \alpha_j \mathbf{T}_j \quad (20)$$

can be directly obtained. For this purpose, the i-th component of the natural response is expressed as

$$x_{hi}(t) = \sum_{j=1}^{n} c_{ij} e^{\lambda_j t}\ ,\ i = 1, \ldots, n. \quad (21)$$

Next, the kth derivative of (21) is taken

$$x_{hi}^{(k)}(t) = \frac{\mathrm{d}^k x_{hi}}{\mathrm{d}t^k} = \sum_{j=1}^{n} \lambda_j^k c_{ij} e^{\lambda_j t}\ ,\ i = 1, \ldots, n. \quad (22)$$

Finally, the following linear equation system is obtained by writing (22) successively for $k = 0, \ldots, n-1$, at time $t = 0$

$$\begin{bmatrix} 1 & 1 & 1 & \cdots & 1 \\ \lambda_1 & \lambda_2 & \lambda_3 & \cdots & \lambda_n \\ \lambda_1^2 & \lambda_2^2 & \lambda_3^2 & \cdots & \lambda_n^2 \\ \vdots & \vdots & \vdots & \ddots & \vdots \\ \lambda_1^{n-1} & \lambda_2^{n-1} & \lambda_3^{n-1} & \cdots & \lambda_n^{n-1} \end{bmatrix} \begin{bmatrix} c_{i1} \\ c_{i2} \\ c_{i3} \\ \vdots \\ c_{in} \end{bmatrix} = \begin{bmatrix} x_{hi}(0) \\ x_{hi}^{(1)}(0) \\ x_{hi}^{(2)}(0) \\ \vdots \\ x_{hi}^{(n-1)}(0) \end{bmatrix}. \quad (23)$$

In the above system, the coefficient matrix is known as the Vandermonde matrix [21], and the right-hand side vector can be recursively obtained by taking the ith component of the sequence of vectors

$$\begin{aligned} \mathbf{x}_h(0) &= \mathbf{x}_0 - \mathbf{x}_f(0) \\ \mathbf{x}_h^{(1)}(0) &= \mathbf{A}\mathbf{x}_h(0) \\ \mathbf{x}_h^{(2)}(0) &= \mathbf{A}\mathbf{x}_h^{(1)}(0) \\ &\vdots \\ \mathbf{x}_h^{(k)}(0) &= \mathbf{A}\mathbf{x}_h^{(k-1)}(0) \\ &\vdots \\ \mathbf{x}_h^{(n-1)}(0) &= \mathbf{A}\mathbf{x}_h^{(n-2)}(0). \end{aligned} \quad (24)$$

Note that this approach is particularly suitable for those applications in which a single element of $\mathbf{x}$ is needed. If conventional LU factorization [22] is employed to solve (23), it should be kept in mind that obtaining subsequent state vector components requires only the forward/backward elimination process to be performed, as the Vandermonde matrix remains constant and the right-hand side vector is readily available.

D. Lagrange Interpolation Formula

In terms of $\mathbf{C}_j$, (17) reduces to

$$\sum_{j=1}^{n} \mathbf{C}_j = \mathbf{x}_h(0). \quad (25)$$

By definition, the eigenvector $\mathbf{C}_j$ satisfies

$$(\mathbf{A} - \lambda_j\mathbf{I})\mathbf{C}_j = 0 \quad (26)$$

and, for any $\lambda_i \neq \lambda_j$, also

$$(\mathbf{A} - \lambda_i\mathbf{I})\mathbf{C}_j = (\lambda_j - \lambda_i)\mathbf{C}_j. \quad (27)$$

Multiplying both sides of (25) by all terms $(\mathbf{A}-\lambda_i\mathbf{I})$, except for $i=j$, and taking into account (26) and (27), yields

$$\prod_{i\neq j}(\mathbf{A}-\lambda_i\mathbf{I})\mathbf{x}_h(0)=\prod_{i\neq j}(\lambda_j-\lambda_i)\mathbf{C}_j \tag{28}$$

or, rearranging

$$\mathbf{C}_j=\left[\prod_{i\neq j}\frac{(\mathbf{A}-\lambda_i\mathbf{I})}{\lambda_j-\lambda_i}\right]\mathbf{x}_h(0) \tag{29}$$

which is known as the Lagrange interpolation formula. Note that, while each solution of (23) provides a row of the similarity transformation matrix, $\mathbf{C}=[\mathbf{C}_1,\mathbf{C}_2,\ldots,\mathbf{C}_n]$, the Lagrange formula constitutes a closed-form expression for each column of $\mathbf{C}$.

The computation of $\mathbf{C}_j$ can be organized as a sequence of matrix-vector products, from right to left, as follows:

$$\mathbf{C}_j=\frac{1}{\prod_{i\neq j}(\lambda_j-\lambda_i)}\left[(\mathbf{A}-\lambda_1\mathbf{I})\ldots[(\mathbf{A}-\lambda_{j-1}\mathbf{I})\ldots [(\mathbf{A}-\lambda_{j+1}\mathbf{I})\ldots[(\mathbf{A}-\lambda_n\mathbf{I})\mathbf{x}_h(0)]]]\right]. \tag{30}$$

Nearly one-half of the computations can be saved when the last state vector component, x_n, is exclusively sought, because in this case only the last $2,3,\ldots n-1$ elements of the intermediate vectors, from left to right respectively in the expression above, are needed to obtain the n-th element of each $\mathbf{C}_j$, as a consequence of $\mathbf{A}$ being a tridiagonal matrix.

For this particular application, an interesting alternative arises to obtain x_n. Let us define an auxiliary row vector $\boldsymbol{\beta}_j$, computed from left to right as follows:

$$\boldsymbol{\beta}_j=\left[\left[\left[\mathbf{e}_n^T(\mathbf{A}-\lambda_1\mathbf{I})\right]\ldots(\mathbf{A}-\lambda_{j-1}\mathbf{I})\right]\ldots (\mathbf{A}-\lambda_{j+1}\mathbf{I})\right]\ldots(\mathbf{A}-\lambda_n\mathbf{I})\right] \tag{31}$$

where $\mathbf{e}_n=[0,0,\ldots,0,1]^T$. Then, the n-th component of each eigenvector $\mathbf{C}_j$ can be simply obtained by performing the inner product

$$c_{nj}=\frac{1}{\prod_{i\neq j}(\lambda_j-\lambda_i)}\left[\boldsymbol{\beta}_j\mathbf{x}_h(0)\right]. \tag{32}$$

Although this way of obtaining c_{nj} is not cheaper than the direct application of (30), a significant computational saving can be achieved if $\boldsymbol{\beta}_j$ is stored when computed for the first time and subsequently retrieved for different initial conditions (see Section VIII).

VI. Example: Transmission Line De-Energization

This section presents an example aimed at comparing the results provided by the distributed parameter model of the EMTP with those obtained by the cascaded connection of lumped-parameter π models. For illustration purposes, the Vandermonde method is employed to determine the respective coefficients c_{ij} of the state-space model, assuming that only the load voltage is required. Except for potential round-off errors, the same results are provided by competing procedures.

The test case, shown in Fig. 3, refers to a 220-kV system comprising a resistive load $R_r=96\ \Omega$, a voltage source with $R_s=2\ \Omega$, $L_s=0.06$ H, and a 100-km transmission line with $R=0.07\ \Omega/\mathrm{km}$, $L=10^{-3}$ H/km, $C=1210^{-9}$ F/km. The conductance of the transmission line is neglected. Initially, the line is in steady-state, fed by a 50-Hz sinusoidal voltage $v_s(t)=220\sqrt{2}\sin(100\pi t)$ kV. At time $t=20$ ms the opening decision is taken and the breaker opens at the next zero current crossing ($t=t_0$). The time evolution of the load voltage, $v_r(t)$, is sought for $t\geq t_0$.

A. Steady State Response

For $t\leq t_0$ the time evolution of the load voltage and source current is obtained by phasor analysis, yielding:

$$v_r(t)=259\,200\sin(100\pi t-0.45)\ \mathrm{V} \tag{33}$$

and

$$i_s(t)=2686\sin(100\pi t-0.41)\ \mathrm{A}. \tag{34}$$

The time instant when the breaker effectively opens can be obtained from

$$i_s(t_0)=2686\sin(100\pi t_0-0.41)=0\Rightarrow t_0=21.3\,\mathrm{ms}. \tag{35}$$

$$\mathbf{A}_l=\begin{bmatrix} 0 & -5\cdot10^6 & & & & & \\ 30 & -70 & -30 & & & & \\ & 2.5\cdot10^6 & 0 & -2.5\cdot10^6 & & & \\ & & 30 & -70 & -30 & & \\ & & & 2.5\cdot10^6 & 0 & -2.5\cdot10^6 & \\ & & & & 30 & -70 & -30 \\ & & & & & 5\cdot10^6 & -5.2\cdot10^4 \end{bmatrix} \tag{36}$$

B. Natural Response

For $t \geq t_0$, i_s should be removed from the state vector. When three nominal π circuits are adopted, the state vector for the system shown in Fig. 3 reduces to

$$\mathbf{x} = [\, v_1 \quad i_1 \quad v_2 \quad i_2 \quad v_3 \quad i_3 \quad v_r \,]^T$$

and the system matrix [see (36) at the bottom of the previous page] whose associated eigenvalues are

$$\begin{aligned} \lambda_1 &= -4.9 \cdot 10^4 \\ \lambda_{2,3} &= -99 \pm j1.7 \cdot 10^4 \\ \lambda_{4,5} &= -523 \pm j1.2 \cdot 10^4 \\ \lambda_{6,7} &= -967 \pm j4.5 \cdot 10^3. \end{aligned} \tag{37}$$

Taking into account that the system is energized for $t < t_0$ with a sinusoidal source, the initial state $\mathbf{x}_0$ can be calculated by phasor analysis techniques, yielding (see equation at the bottom of the page).

Solving the linear system (23) for $i = 7$ provides the following $\{c_{ij}\}$ coefficients:

$$\begin{aligned} &c_{71} = 1590 \\ &c_{72} = -161.15 - j234.48 \;;\; c_{73} = -161.15 + j234.48 \\ &c_{74} = 64.83 + j1228 \;;\; c_{75} = 64.83 - j1228 \\ &c_{76} = -6087.64 - j9840.14 \,;\, c_{77} = -6087.64 + j9840.14. \end{aligned} \tag{38}$$

Therefore,

$$\begin{aligned} v_r(t) = {} & 1590e^{-4.9\cdot10^4(t-t_0)} \\ & + (-161.15 - j234.48)e^{(-99+j1.7\cdot10^4)(t-t_0)} \\ & + (-161.15 + j234.48)e^{(-99-j1.7\cdot10^4)(t-t_0)} \\ & + (64.83 + j1228)e^{(-523+j1.2\cdot10^4)(t-t_0)} \\ & + (64.83 - j1228)e^{(-523-j1.2\cdot10^4)(t-t_0)} \\ & + (-6087.64 - j9840.14)e^{(-967+j4.5\cdot10^3)(t-t_0)} \\ & + (-6087.64 + j9840.14)e^{(-967-j4.5\cdot10^3)(t-t_0)} \end{aligned} \tag{39}$$

or, simplifying the above expressions

$$\begin{aligned} v_r(t) = {} & 1590e^{-4.9\cdot10^4(t-t_0)} \\ & - 569e^{-99(t-t_0)}\cos(1.7 \cdot 10^4(t-t_0) + 0.97) \\ & + 2459.4e^{-523(t-t_0)}\cos(1.2 \cdot 10^4(t-t_0) + 1.52) \\ & - 23\,142.1e^{-967(t-t_0)}\cos(4.5 \cdot 10^3(t-t_0) + 1.02). \end{aligned} \tag{40}$$

The solution obtained with three cascaded nominal π circuits compares well with that provided by EMTP (see Fig. 6).

Fig. 7 shows an even better agreement for five cascaded nominal π circuits. For ten or more π sections both curves virtually superpose.

The line energization problem, omitted because of space limitations, is solved in a similar manner, the major difference being the additional state variable associated with the source inductance, i_s.

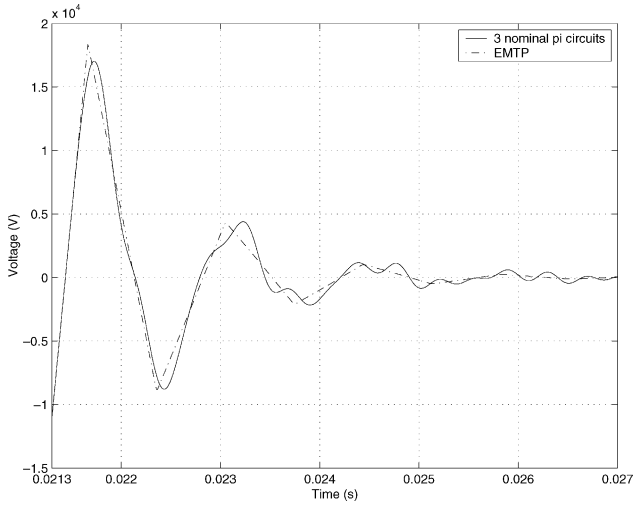

Fig. 6. Natural response with three nominal π circuits and EMTP.

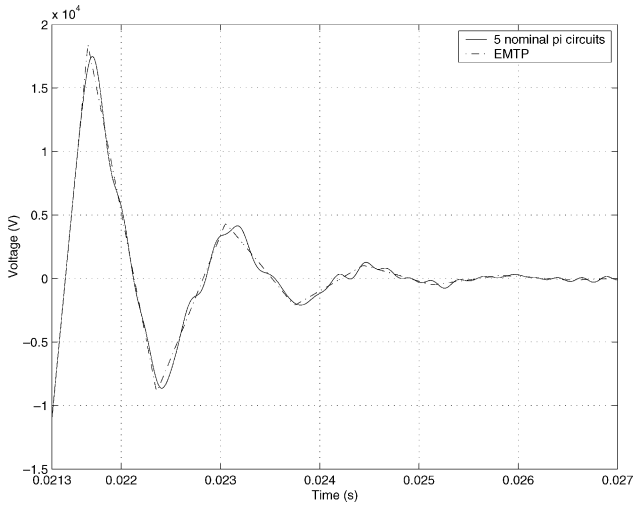

Fig. 7. Natural response with five nominal π circuits and EMTP.

VII. Computational Cost

In this section, a comparison of the computational cost involved in the computation of $\mathbf{x}_h(t)$ during the line de-energization is presented. The total number of floating point operations, or flops, is used. Any arithmetic operation on real arguments generates a flop. With complex arguments, each multiplication/division generates six flops, while an addition/subtraction generates two flops.

For the following comparative analysis, the reader is referred to data presented in Tables I and II, regarding the computational cost of common matrix-vector operations.

$$\mathbf{x}_0 = \mathbf{x}_h(0) = [\, 73\,902.4 \quad -31.2 \quad 43\,680 \quad -58.2 \quad 15\,574 \quad -112.3 \quad -10\,778 \,]^T.$$

TABLE I
FLOPS INVOLVED IN THE SOLUTION STEPS OF LINEAR EQUATION SYSTEMS

Matrix type	LU factorization	Forward & backward
Real tridiagonal	$3n-3$	$5n-4$
Complex tridiagonal	$14n-14$	$20n-14$ (eig. problem)
Real dense	$\frac{2}{3}n^3-\frac{1}{2}n^2-\frac{1}{6}n$	$2n^2-n$

TABLE II
FLOPS INVOLVED IN A MATRIX-VECTOR MULTIPLICATION

Matrix type	Vector type	Flops
Real tridiagonal	Real	$5n-4$
Complex tridiagonal	Complex	$22n-16$

A. EMTP-Based Solution

In order to obtain the receiving-end voltage for the line shown in Fig. 3, it is necessary to build and solve the nodal equations

$$\begin{bmatrix} \frac{1}{Z} & 0 \\ 0 & \frac{1}{Z}+\frac{1}{R_r} \end{bmatrix} \begin{bmatrix} v_1(t) \\ v_r(t) \end{bmatrix} = \begin{bmatrix} I_s(t) \\ I_r(t) \end{bmatrix} \tag{41}$$

and then to obtain line currents $i_r(t)$ and $i_s(t)$ that will be needed at instant $t+\tau$, [16]

$$\begin{aligned} i_s(t) &= \tfrac{v_1(t)}{Z} - I_s(t) \\ i_r(t) &= \tfrac{v_r(t)}{Z} - I_r(t) \end{aligned}. \tag{42}$$

Hence, a total of 18 flops/step are required, plus several additional flops at the beginning to compute constant coefficients. Note that the sending-end voltage is also required, and that electrical magnitudes at intermediate points can not be obtained unless the line is split appropriately.

B. Trapezoidal Rule

Equation (13) can be rewritten for the zero-input case as

$$\left(\mathbf{I}\frac{2}{\Delta t}-\mathbf{A}\right)\mathbf{x}_{k+1} = \left(\mathbf{I}\frac{2}{\Delta t}+\mathbf{A}\right)\mathbf{x}_k. \tag{43}$$

Assuming the same step size is used throughout the process, the computational cost consists of the following terms.

- Preliminary phase: $2n$ additions to obtain the matrices at both sides of (43) plus the LU factorization of the coefficient matrix.
- Each step: Matrix-vector multiplication on the right-hand side plus the forward/backward solution stage.

This yields a total of $5n-3$ flops for the preliminary phase and $10n-8$ flops per iteration. Note the resulting linear cost, owing to the special nonzero pattern of A,

The number of iterations depends both on the step size and duration of the transient period. A reasonable step size for the above example is 10^{-5} s, which means that the first 5 ms involve 500 simulation steps. Table III summarizes the total flops required by the numerical integration approach for the computation of the line de-energization. As discussed in Section V, there is virtually no saving if only the receiving-end voltage, $x_n(t)$, is needed.

C. Eigensystem-Based Solution

This and the remaining procedures require that the system eigenvalues be available. Experience reveals that, for the kind of circuits considered in this paper, at most two eigenvalues are real. Therefore, for simplicity of analysis, it will be assumed that all eigenvalues are complex in order to evaluate the computational cost of the different methods. According to [23], obtaining the eigenvalues of a tridiagonal matrix by means of the *TLR* algorithm involves about $25n^2$ flops. This iterative scheme applies implicit double shift *LR* iterations to the scaled tridiagonal matrix until all the eigenvalues are found.

Apart from obtaining the eigenvalues, the following computations are necessary.

- Eigenvectors: Computing each of the $n/2$ eigenvectors (the rest are complex conjugate) involves building and factorizing the coefficient matrix of (19). As this matrix is singular, a zero pivot will be eventually detected. This pivot and the respective element of the right-hand side vector are set to 1, allowing $\mathbf{T}_j$ to be subsequently solved by forward/backward elimination [24]. The total number of flops required to obtain the eigenvectors is $18n^2-14n$.
- Vector $\boldsymbol{\alpha}$: Taking advantage of the eigenvector's complex conjugate symmetry, this column vector can be obtained by rewriting (18) as a real-coefficient equation system with an extra cost of n flops. The total number of flops to obtain $\boldsymbol{\alpha}$ in this way is $(2/3)n^3+(3/2)n^2-(1/6)n$.
- If all state variables are needed, $3n^2$ flops should be added to account for the products $\boldsymbol{\alpha}_j\mathbf{T}_j$ in (16). On the other hand, only $3n$ additional flops are required to obtain a single component of the state vector.

The total cost for this procedure is shown in Table III (all variables) and Table IV (single variable) for different n values.

D. Vandermonde Matrix

The following items determine the computational cost in this case, in addition to the computation of the eigenvalues.

- Assuming pairs of complex conjugate eigenvalues, obtaining the Vandermonde matrix requires $n(n-1)/2$ complex multiplications (i.e., $3n^2-3n$ flops).
- Computing the entire set of terms $x_h^{(k)}(0)$ by the sequence (24) involves $5n^2-9n+4$ flops.
- Taking advantage of the complex conjugate symmetry, the system of (23) can be also rewritten in terms of a real matrix, which is factorized only once.
- As many forward/backward elimination processes as wanted state variables are performed to obtain the respective coefficients c_{ij}.

Table III shows the total cost associated to this procedure. It is worth noting the low cost that results when a single state variable is sought (Table IV).

E. Lagrange Interpolation Formula

Besides the computation of the eigenvalues, this approach involves the following preliminary steps.

• Computation of matrices $\mathbf{A}-\lambda_i\mathbf{I}$ ($2n$ flops each).

TABLE III
TOTAL FLOPS REQUIRED TO OBTAIN ALL STATE VARIABLES FROM SCRATCH

	Trapezoidal	Eigensystem	Vandermonde	Lagrange
n	$5n-3+500(10n-8)$	$\frac{2}{3}n^3+\frac{95}{2}n^2-\frac{85}{6}n$	$11n^3+\frac{115}{8}n^2+\frac{7}{4}n$	$11n^3+\frac{115}{8}n^2+\frac{7}{4}n$
7	31032	2457	2377	4342
12	56057	7822	9002	20667
22	106107	29777	43377	122672

- Taking advantage of the complex conjugate symmetry, only $n(3n-2)/8$ terms of the form $\lambda_j-\lambda_i$ in **(29)** need to be computed.

Next, computing each of the $n/2$ column vectors $\mathbf{C}_j$ comprises the following steps:

- The product of $n-1$ terms $\lambda_j-\lambda_i$ which is then used to scale $\mathbf{x}_h(0)$.
- If all state variables are wanted then $n-1$ matrix-vector products are required. As discussed above, if only the receiving-end bus voltage, $x_n(t)$, is needed, just one component of the last matrix-vector product, two components of the previous product, and so on are necessary.

Table III shows the total cost associated to this procedure, including the computation of eigenvalues (see Table IV for the single variable case).

F. Comparison

In view of Tables III and IV, the following conclusions can be drawn, as far as state-space solution approaches are concerned:

- For the size of integration steps required in practice, the trapezoidal rule is much more expensive than competing methods based on explicitly obtaining each natural mode, particularly for long-lasting transients.
- The Vandermonde matrix approach is most appropriate when a single state variable is needed.
- When the entire state vector is wanted, the eigenvector-based method is slightly cheaper.

The cost corresponding to the EMTP is included only in Table IV, as the EMTP solution method does not allow the evolution of intermediate variables to be obtained. For a transient lasting 5 ms, like that of the example, the EMTP is more expensive than the Vandermonde scheme with 12 state variables. Longer transients make eigenvalue-based approaches, whose computational cost is independent of the simulation period, more competitive.

Figures shown in Tables III and IV may be significantly affected by the presence of nonlinear elements and switching devices, which may force the step size to be changed and/or eigenvalues to be recomputed, depending on the solution approach. Analyzing all these cases is however a cumbersome task, beyond the space limitations of a single paper.

TABLE IV
TOTAL FLOPS REQUIRED TO OBTAIN THE RECEIVING-END VOLTAGE FROM SCRATCH

	EMTP	Eigensystem	Vandermonde	Lagrange
n	9000	$\frac{2}{3}n^3+\frac{89}{2}n^2-\frac{67}{6}n$	$\frac{11}{2}n^3+\frac{223}{8}n^2-\frac{23}{4}n$	$\frac{11}{2}n^3+\frac{223}{8}n^2-\frac{23}{4}n$
7	9000	2331	1831	3100
12	9000	7426	5966	13137
22	9000	28391	23511	70917

VIII. REPEATED SOLUTIONS

In practice, it is very unlikely that a single transient analysis is performed. Most frequently, repeated solutions are carried out aimed at finding worst-case situations (e.g., when statistically characterizing switching overvoltages). Typically, the only difference among different simulation scenarios lies in the initial conditions $\mathbf{x}_h(0)$.

In such cases, the Lagrange interpolation formula constitutes the cheapest approach to obtain a single state variable by means of (32), provided the coefficients $\boldsymbol{\beta}_j$ are available from previous runs.

Table V compares the cost involved in subsequent computations of the receiving-end voltage for the same line configuration and different initial conditions.

It is worth noting that, as updating a single variable by means of the Lagrange formulation involves just n inner products, the EMTP is not competitive for this type of repeated solutions, unless the number of π sections is very high and the simulation period very short. This applies not only to the single line case analyzed in this paper but to systems with arbitrary topologies.

IX. CONCLUSIONS

In this paper, several techniques to analytically obtain the transient response of transmission lines have been reviewed and compared. Assuming frequency-independent parameters, the transmission line is modeled by the cascaded connection of a number of lumped-parameter π circuits. State space equations of the resulting system are written using inductor currents and capacitor voltages as state variables. Once the respective eigenvalues are computed, explicit time evolution

TABLE V
FLOPS REQUIRED TO OBTAIN THE RECEIVING-END VOLTAGE FOR AN ALTERNATIVE SET OF INITIAL CONDITIONS

	EMTP	Trapezoidal	Eigensystem	Vandermonde	Lagrange
n	9000	$500(10n-8)$	$\frac{2}{3}n^3+\frac{3}{2}n^2+\frac{17}{6}n$	$7n^2-10n+4$	$2n^2+2n$
7	9000	31000	322	277	112
12	9000	56000	1402	892	312
22	9000	106000	7887	3172	1012

of the state vector can be obtained by one of the following methods: 1) eigenvector computation followed by the solution of a linear equation system involving the similarity transformation matrix; 2) solution of a linear equation system involving the Vandermonde matrix; and 3) application of the Lagrange explicit formula for each eigenvector. Even though these methods are relatively well known in linear time-invariant circuit analysis, the way they are formulated and applied in this paper, particularly concerning the application of the Lagrange expression for repeated solutions, is original.

The state-space direct approach is first applied to the de-energization of a 50-Hz, 220-kV transmission line, the results showing good agreement with those provided by EMTP simulations, particularly as the number of π sections adopted for the line model increases.

An exhaustive analysis of the computational cost for each method, including the trapezoidal rule for comparison, is performed. It can be concluded that explicitly obtaining the state vector is computationally much less demanding than the trapezoidal rule for the single line case considered in this paper. For a reasonable number of π sections, the Vandermonde method is even cheaper than the EMTP when a single variable is of interest.

Approaches based on the state-space formulation remain valid for linear networks with arbitrary topology, as state-space equations can be always obtained and solved in a systematic manner. However, assessing their computational cost in the general case, particularly the component related to the computation of eigenvalues, constitutes a cumbersome task. Anyway, the main advantage of the state-space formulation is that it provides explicit expressions for the variables of interest in terms of natural frequencies, including intermediate points, rather than a set of discrete-time numerical values. Its main drawback, apart from the bandwidth limitation, is that it can be applied only to circuits which can be assumed to be linear for a given time interval.

Attention is also paid to those cases in which repeated solutions are needed for different sets of initial conditions, for which the Lagrange formula clearly surpass other methods, including the EMTP. Interestingly, the Lagrange expression for repeated solutions developed in this paper is of application to general linear circuits, provided the number of simulations compensates for the cost of the first complete solution.

Although the proposed method has been worked out just for single-phase lines, it can be applied to each propagation mode of multiphase lines.

REFERENCES

[1] J. P. Bickford and M. H. Abdel-Rahman, "Application of travelling wave methods to the calculation of transient-fault currents and voltages in power-system networks," *Proc. Inst. Elect. Eng.*, vol. 3, pp. 153–168, 1980.

[2] H. Dommel, "Digital computer solution of electromagnetic transients in single and multiple networks," *IEEE Trans. Power App. Syst.*, vol. 88, Apr. 1969.

[3] P. Moreno, R. Rosa, and J. L. Naredo, "Frequency domain computation of transmission line closing transients," *IEEE Trans. Power Delivery*, vol. 6, pp. 275–281, 1991.

[4] A. S. AlFuhaid and M. M. Saied, "A method for the computation of fault transients in transmission lines," *IEEE Trans. Power Delivery*, vol. 2, pp. 288–297, 1988.

[5] R. M. Nelms, G. B. Sheble, S. R. Newton, and L. L. Grigsby, "Using a personal computer to teach power system transients," *IEEE Trans. Power Syst.*, vol. 4, pp. 1293–1297, Aug. 1989.

[6] L. A. Shankland, J. W. Feltes, and J. J. Burke, "The effect of switching surges on 34.5 kV system design and equipment," *IEEE Trans. Power Delivery*, vol. 5, pp. 1106–1112, Apr. 1990.

[7] A. Carvalho, M. Lacorte, and O. Knudsen, "Improved ehv line switching surge control by application of mo-arresters and controlled switching," in *Proc. IEEE EMPD '99*, vol. 1, Nov. 1995, pp. 292–297.

[8] M. M. Saied, "On the analysis of capacitor switching transients," in *Proc. IEEE PowerCon 2002*, vol. 1, Oct. 2002, pp. 134–138.

[9] A. P. S. Meliopolulos and C.-H. Lee, "An alternative method for transient analysis via wavelets," *IEEE Trans. Power Delivery*, vol. 15, pp. 114–121, Jan. 2000.

[10] A. T. Johns, Z. Q. Bo, Y. H. Song, and R. K. Aggarwal, "Spectrum analysis of fault-induced transients for the development of protection equipment," in *Proc. IEE 2nd Int. Conf. Advances in Power System Control, Operation and Management*, 1993, pp. 72–76.

[11] B. Jeyasurya, T. H. Vu, and W. J. Smolinski, "Determination of transient apparent impedances of faulted transmission lines," *IEEE Trans. Power App. Syst.*, vol. 102, pp. 3370–3378, Oct. 1983.

[12] A. Greenwood, *Electrical Transients in Power Systems*. New York: Wiley, 1991.

[13] J. R. Martí, L. Martí, and H. W. Dommel, "Transmission line models for steady-state and transient analysis," in *Proc. IEEE/NTVA Athens Power Tech Conf.*, Athens, Greece, Sep. 1993.

[14] R. M. Mathur and X. Wang, "Real-time digital simulator of the electromagnetics transients," *IEEE Trans. Power Delivery*, vol. 4, Apr. 1989.

[15] Y. Tang, H. Chen, H. Wang, F. Dai, and S. Jiang, "Transmission line models used in travelling wave studies," in *Proc. IEEE Transmission Distribution Conf.*, vol. 2, 1999, pp. 797–803.

[16] N. Watson and J. Arrillaga, *Power Systems Electromagnetic Transient Simulation*. London, U.K.: The Institution of Electrical Engineers, 2003, vol. 39, IEE Power and Energy Series.

[17] C. Moler and C. V. Loan, "Nineteen dubious ways to compute the exponential of a matrix," *SIAM Rev.*, vol. 20, no. 4, pp. 801–836, 1978.

[18] D. E. Johnson, J. R. Johnson, and J. L. Hilburn, *Electric Circuit Analysis*. Englewood Cliffs, NJ: Prentice-Hall, 1992.

[19] A. B. Carlson, *Circuits*. New York: Thomson, 2000.

[20] R. K. Nagle, E. B. Saff, and A. D. Snider, *Fundamentals of Differential Equations*. Reading, MA: Addison-Wesley, 2000.
[21] J. H. Wilkinson, *The Algebraic Eingenvalue Problem*. Oxford, U.K.: Oxford Univ. Press, 1965.
[22] G. H. Golub and F. V. Loan, *Matrix Computations*. Baltimore, MD: Johns Hopkins Univ. Press, 1989.
[23] G. A. Geist, "Reduction of a general matrix to tridiagonal," *SIAM J. Matrix Analysis and Applications*, vol. 12, no. 2, pp. 362–373, 1999.
[24] M. S. Mamis and M. Köksal, "Solution of eigenproblems for state-space transient analysis of transmission lines," *Elect. Power Syst. Res.*, vol. 55, pp. 7–14, 2000.

Jose A. Rosendo Macías (M'04) was born in Carmona, Spain, in 1968. He received the electrical engineering and the Ph.D. degree from University of Sevilla, Sevilla, Spain.

He is currently Associate Professor at the Department of Electrical Engineering, University of Sevilla. His research interests include circuits theory, power systems analysis, digital signal processing, and digital relaying.

Antonio Gómez Expósito (F'05) was born in Spain in 1957. He received the electrical and doctor engineering degrees from the University of Seville, Seville, Spain.

Since 1982, he has been with the Department of Electrical Engineering, University of Seville, where he is currently a Professor and Head of the Department. His primary areas of interest are optimal power system operation, state estimation, and computer relaying.

Alfonso Bachiller Soler (M'05) was born in Guadalajara, Spain, in 1973. He received the electrical engineering degree from the University of Sevilla, Sevilla, Spain, in 1998.

He is currently Assistant Professor at the Department of Electrical Engineering, University of Sevilla. His research interests include circuits theory, power systems analysis, and electric machinery.